MUST Journal of Research and Development (MJRD) Volume 7 Issue 3, July-September 2026
e-ISSN: 2683-6467 & p-ISSN: 2683-6475

Mathematical Analysis of Mpox in Human Population: The Effects of Vaccination Strategies

Mlyashimbi Helikumi[a], Philipina Shayo[b] and Herman Trazias[a]

[a]*Department of Mathematics, Mbeya University of Science and Technology, Mbeya, Tanzania*
[b]*Department of Earth Science,Mbeya University of Science and Technology, Mbeya, Tanzania*
DOI: 10.62277/mjrd2026v7i30003

ARTICLE INFO

Keywords:
Article History:
Received: 20^{th} November 2025
Revised: 10^{th} February 2026
Accepted: 10^{th} March 2026
Published: 30^{th} August 2026

Keywords:
Monkeypox virus
model formulation
Disease transmission
parameter estimation
first and second-dose vaccination

ABSTRACT

In this research work, a fractional-order model of monkeypox disease transmission within the human population is formulated and studied. The formulated model incorporates two control strategies namely; vaccination and health education campaign. In model analysis, the disease free-equilibrium and basic reproduction number, are computed. The existence and uniqueness of model solution using fixed point theorem have been analyzed. Meanwhile, the global stability of the model have been performed using well formulated Lyapunov function and the results showed that the model is stable when $\mathcal{R}_0 < 1$ and unstable when $\mathcal{R}_0 > 1$. In model simulations, parameter estimation using reported cases of monkeypox disease from Democratic Republic of Congo have been performed to compare the results for fractional ($z = 0.5$) and integer ($z = 1$) order derivatives. The results showed that fitting the model at $z = 0.5$ had good results compared to when $z = 1$. Implying that fractional model presented good results compared to integer-order derivatives. Besides, we performed Sensitivity analysis of the basic reproduction number using computed partial rank correlation coefficients to investigate the impact of each parameter on the disease transmission. Furthermore, we performed numerical simulation of the model to assess the impact of memory effects on the spread of monkeypox virus transmission in the population. Additionally, numerical simulation to investigate the effects of health education and vaccination was performed. Overall, the results showed that when the efficacy of first-dose vaccination was changed from 75% to 95% and the rate of health education campaign retained at 0.1 the threshold quantity $\mathcal{R}_0$ remained greater than unity. In contrast when the efficacy of first-dose vaccination was changed from 75% to 95% and the rate of health education campaign changed from 0.1 to 0.9 the threshold quantity $\mathcal{R}_0$ was observed to be less than unity. The results have implication that the efficacy of first-dose vaccination must be greater than 95% and rate of health education campaign must be greater that 0.9 for the disease to eliminated in the population Monkeypox virus (MPXV) transmission remains an important public health concern, particularly in populations where vaccination coverage, disease surveillance, and access to effective preventive measures are limited. Mathematical modelling provides a valuable framework for understanding MPXV transmission dynamics and assessing the effectiveness of control interventions by describing the interactions among susceptible, vaccinated, exposed, and infectious populations. In particular, incorporating first- and second-dose vaccination into transmission models allows the differential protection provided by successive vaccine doses to be examined, together with vaccination rates and vaccine efficacy. Parameter estimation using reported MPXV cases is essential for calibrating the model and improving its ability to describe observed disease patterns. Such models can also be used to determine key epidemiological quantities, including the basic reproduction number, and to evaluate the effects of vaccination and other interventions on disease transmission. Therefore, integrating MPXV model formulation, parameter estimation, and first- and second-dose vaccination provides a useful mathematical framework for identifying effective control strategies and establishing conditions under which MPXV transmission can be reduced and potentially eliminated from the population.

[*]**Corresponding author's e-mail address: mhelikumi@yahoo.co.uk** (Helikumi, M)

1. Introduction

The Mpox virus (MPXV) causes the zoonotic disease Mpox, infecting both humans and animals Mandja et al. (2019). The virus is naturally endemic to Central and West Africa, with countries like the Benin, Cameroon, the central African republic, the Democratic Republican of the Congo, Gabon, Ivory Coast, Liberia, Nigeria, Sierra Leone, and South Sudan being the most frequently affected Hatami et al. (2023). Historically, most human Mpox infections were zoonotic, meaning they resulted from contact with infected animals like rodents and non-human primates Banuet-Martinez et al. (2023). Human-to-human transmission was usually limited, mostly occurring within households or small local groups El-Mesady et al. (2022). However, this established pattern shifted dramatically in May 2022, when the first infections of a new multi-country outbreak were reported in the United Kingdom, Portugal, and Spain Farman et al. (2025). The Mpox outbreak quickly spread around the globe, first appearing across Europe and North America, and then rapidly moving into South America, Asia, Oceania, and the Middle East Alakunle et al. (2020). This massive expansion meant that by July 2023, confirmed cases had been reported in over 108 countries, representing a spread far beyond the disease's historic boundaries Mandja et al. (2019). After a person is infected with Mpox, the time before symptoms begin (the incubation period) generally falls within 7 to 17 days Ayeh et al. (2024). When the illness manifests, the typical symptoms include fever, headaches, body aches, and chills. These often precede or accompany swollen lymph glands and the signature skin rash Di Gennaro et al. (2022). The transmission cycle of MPXV is presented in Figure (1):

Mathematical models are essential tools because they allow researchers to investigate and answer complex questions that would be too difficult, costly, or impractical to investigate using real-world methods Lusekelo et al. (2023); McKenzie et al. (2012). A recent example of this is the development and study of Monkeypox disease models, which have been used to explore the potential impact of control strategies like vaccination, health education campaign, and quarantine Peter et al. (2022). Mathematical models of Monkeypox disease transmission and control strategies have been formulated and studies, for more information can refer the readers to Adel et al. (2023); Adepoju & Ibrahim (2024); Alshehri & Ullah (2023); Helikumi et al. (2025); Musafir et al. (2024); Rashid et al. (2025); Soni and Sinha (2024) and the references are therein. Despite efforts to control the spread of Mpox, several challenges remain. One major limitation in mathematical modeling of Mpox disease transmission is a knowledge gap concerning the effectiveness of vaccination in controlling human-to-human transmission Helikumi et al. (2023). This is compounded by the fact that most published models have focused solely on the impact of other measures, such as quarantine, health education, and improved hygiene practices transmission.(see,Adel et al. (2023); Alqahtani et al. (2023); Biswas et al. (2023); Liu et al. (2023); Venkatesh et al. (2024); Yaga (2025); Yuan et al. (2022)) and references are therein. Alqahtani et al. (2023) Vaccination is a critical strategy for controlling Monkeypox, as it provides both pre-exposure and post-exposure prophylaxis, effectively preventing infection, significantly reducing disease severity in breakthrough cases, and helping to contain outbreaks by establishing herd immunity within targeted risk populations Khan et al. (2022); Spath et al. (2022). To curb the global transmission of Mpox, three vaccines have recently been authorized for public use: JYNNEOS (MVA-BN), LC16M8, and ACAM2000 Helikumi et al. (2025). While these tools are essential for disease control, their specific recommendations vary; JYNNEOS (MVA-BN) and LC16M8: Both received approval from the World Health Organization (WHO) and played a vital role in managing outbreaks between 2022 and 2025 Alshehri & Ullah (2023). Because of their safety profiles, they are the preferred options for immunocompromised individuals. The ACAM2000 vaccine was approved in Japan and is specifically prioritized for children under the age of five years Khan et al. (2022). Despite the availability of these medical interventions, achieving total elimination of the virus remains a significant challenge. A primary obstacle is waning population immunity, which complicates long-term prevention efforts and leaves communities vulnerable to resurgence Helikumi et al. (2024). Following the global cessation of routine smallpox vaccination around 1980, the population's historical cross-protection against orthopoxviruses like Monkeypox has steadily declined Helikumi et al. (2023); Khan et al. (2022). This diminishing level of herd immunity has created a large, growing pool of susceptible individuals worldwide in using vaccination as mpox control measure, and hence poses a growing public health threats Brand et al. (2023); Spath et al. (2022).

Recently, Mathematical models incorporating fractional order differential equations have gained significant attention (seeGhanbari & Atangana (2020); Nisar et al. (2024); Rakkiyappan et al. (2019)), and offer accurate results in disease modeling compared to integer-order derivatives. The most common fractional-order derivatives used in dynamical systems include Caputo, Caputo-Fabrizio and Atangana-Baleanu derivatives Helikumi and Lolika (2022). These fractional calculus differ mainly in the way how they employ memory kernel which govern how the past states influence the present state in the biological systems Podlubny (1999). It is worth mentioning that, fractional order derivatives have several advantages over classical-order operators, as they effectively capture hereditary properties, long-range interactions, and memory effects present in biological systems Nisar et al. (2024). Additional, in dynamical systems the present state of population is often

Figure 1: *Transmission cycle of monkeypox disease dynamics* Mandja et al. (2025)

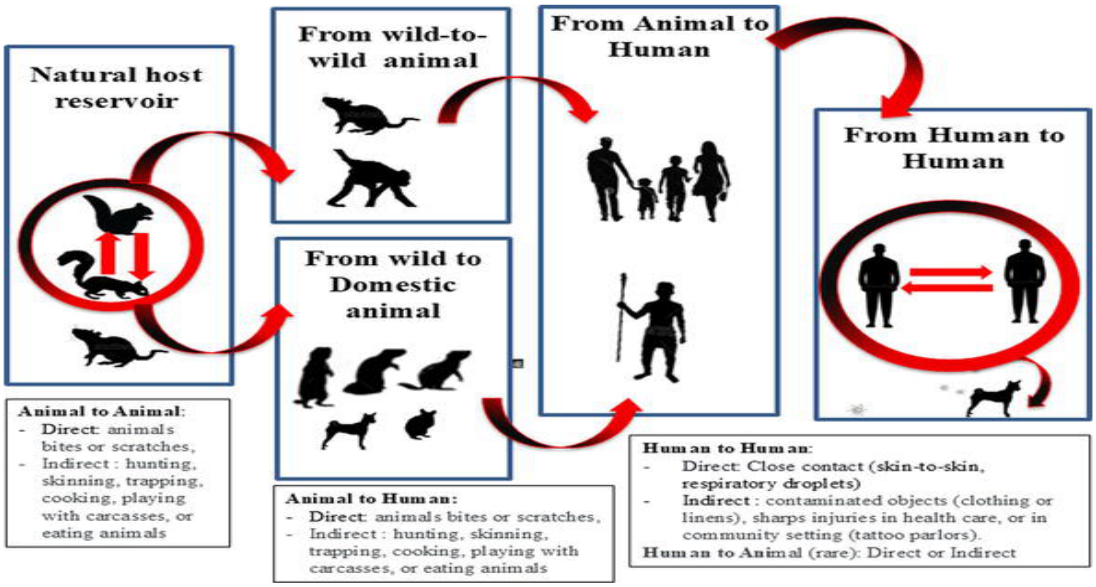

influenced by not only its current state but also its entire history of interactions Rakkiyappan et al. (2019). In contrast, classical integer-order derivatives assume that the system's future depends only on the current state, and thereby ignore the long term effects Yaga (2025).

Motivated by the above discussion, this study aim to investigate the effects of vaccination strategies on monkey pox transmission dynamics. To the best of our knowledge non-of fractional-order model for monkey pox transmission formulated and incorporated human awareness, early and post-vaccination strategies. Therefore in this study, we propose a fractional-order model using Caputo derivatives and assess the effects of health education campaign and vaccination on minimize the spread of Monkeypox disease in the population.

The rest of the paper is organized as follows: in Section 2, mathematical model formulation is presented, in Section 3, model analysis presented; positivity of variables and boundedness of trajectories are presented, computation of reproduction number and existence of model solutions are presented in section 4, results and discussion is presented in section 5, and conclusion remarks complete the paper in Section 6.

2. Model Formulation

In this section, we stratify the human population into seven mutually exclusively based on the health status of states: we denote the Maternally new born babies from first day to six months by $M(t)$, susceptible individuals who are at risk of contracting the smallpox disease $S(t)$, exposed individuals $E(t)$, individuals who have received first dose vaccination $V_1(t)$, individuals received second dose vaccination $V_2(t)$, infected individuals and infectious $I(t)$, and recovered humans $R(t)$. Thus, the total population of human at time t is denoted by $N_h(t)$ given as:

$$N(t) = M(t) + S(t) + V_1(t) + V_2(t) + E(t) + I(t) + R(t) \quad (1)$$

Furthermore, we considered all parameters and variables of the proposed model to be non-negative, and the parameters are defined as follows: Λ denotes the new recruitment rate of maternally immunized babies, and we assumed that new inborn neonates are born with immune system joining the group of vaccinated individuals who have received first dose vaccination at the rate θ. The parameter p (with $0 \leq p \leq 1$) denotes the proportional of new born babies who migrate to vaccinated class and $(1-p)$ represent the group of newborn babies who have lost immunity within six months and migrate to naiver susceptible class. Susceptible individuals receive the first dose vaccination at the rate of ω_1 and join vaccinated class, while individuals who receive second dose vaccination at the rate ω_2 develop permanent immunity and join recovered class at the rate γ_2. Naive susceptible, individuals received first and those who received second dose vaccination decrease through infection at the rate βSI, $\beta V_1 I$, and $\beta V_2 I$ respectively. The parameter β represents the probability of disease transmission following successful contact between healthy and infected individuals; Despite the fact that, both naive susceptible, individuals received the first and second dose vaccination have the same probability of getting the Mpox infection whenever they contact with infected individuals, the parameters ϵ_1 and ϵ_2 denote the reduction factor on the disease transmission for individuals received first and second dose

vaccination. η denotes the health education campaigns on smallpox disease transmission. Besides, humans who exposed to the Mpox virus disease become infectious at the rate α, and those with clinical symptoms receive treatment and recover at γ_1. Furthermore, individuals who have received their second vaccine dose possess a comprehensive understanding of Mpox transmission and the necessary precautions to take when interacting with infected persons. Consequently, it is assumed that some of humans who received second dose vaccination join in recovered class at the rate γ_2. Based on the above assumptions, we have assumed the following flow chart and non-linear differential equations: From the flowchart diagram in Fig.(2), the dynamics of

Figure 2: Model flowchart illustrating the dynamics of Mpox disease transmission

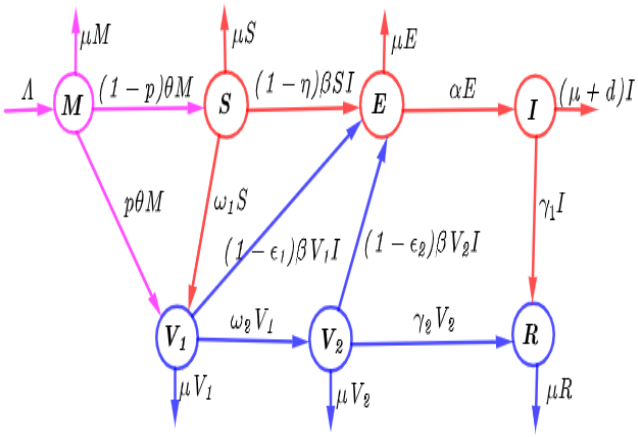

interaction between humans is given by the following system of fractional differential equations:

$$\begin{cases} {}^{c}_{t_0}D^{z}_{t} M(t) & = \Lambda - (\theta+\mu)M(t), \\ {}^{c}_{t_0}D^{z}_{t} S(t) & = (1-p)\theta M(t) - (1-\eta)\beta S(t)I(t) - \\ & \quad (\omega_1+\mu)S(t), \\ {}^{c}_{t_0}D^{z}_{t} V_1(t) & = p\theta M(t) + \omega_1 S(t) - \\ & \quad (1-\epsilon_1)\beta V_1(t)I(t) - (\mu+\omega_2)V_1(t) \\ ds\,{}^{c}_{t_0}D^{z}_{t} V_2(t) & = \omega_2 V_1(t) - (1-\epsilon_2)\beta V_2(t)I(t) - \\ & \quad (\mu+\gamma_2)V_1(t) \\ {}^{c}_{t_0}D^{z}_{t} E(t) & = (1-\eta)\beta S(t)I(t) + \\ & \quad (1-\epsilon_1)\beta V_1(t)I(t) + \\ & \quad (1-\epsilon_2)\beta V_2(t)I(t) - (\mu+\alpha)E(t), \\ ds\,{}^{c}_{t_0}D^{z}_{t} I(t) & = ds\,\alpha E(t) - (\mu+\gamma_1)I(t), \\ {}^{c}_{t_0}D^{z}_{t} R(t) & = \gamma_2 V_2(t) + \gamma_1 I(t) - \mu R(t). \end{cases} \quad (2)$$

3. Model Analysis

3.1. Preliminaries on the Caputo Fractional Calculus

We begin by introducing the definition of Caputo fractional derivative and state related theorems (see, Caputo (1967); Diethelm (2010); Vargas-De-LeÃşn (2015)) that we will utilise to derive important results in this work.

Definition 3.1. *Suppose that $z > 0, t > a, za, t \in \mathbb{R}$. The Caputo fractional derivative is given by*

$${}^{c}_{0}D^{z}_{t} f(t) \frac{1}{\Gamma(n-zi)} \int_a^t \frac{f^n(\xi)}{(t-\xi)^{z+1-n}} d\xi, \quad (3)$$

$n-1 < \phi, n \in \mathbb{N}$.

Definition 3.2. *(Caputo derivative of a constant Diethelm (2010)). The fractional derivative for a constant function $f(t) = c$ is zero, that is,*

$${}^{c}_{0}D^{z}_{t} c = 0, \qquad z \in (0,1) \quad (4)$$

Definition 3.3. *The Caputo-fractional derivative in Liouvile-Caputo sense is defined as*

$${}^{c}_{0}D^{z}_{t} f(t) = \frac{N(z)}{1-\phi} \int_0^t f'(\tau) exp\left[\frac{z(t-\tau)}{1-\tau}\right] d\tau \quad (5)$$

where by $N(z)$ is normalized function such as $N(0) = N(1) = 1$.

Definition 3.4. *The Caputo-fractional integral of order $q(0 < z \leq 1)$ of the function $f(t)$ is defined as*

$$\begin{aligned} {}^{c}_{0}I^{z}_{t} f(t) &= \frac{2(1-z)}{(2-z)N(z)} f(t) + \\ & \quad \frac{2z}{(2-z)N(z)} \int_0^t f(s) ds, \quad t \geq 0, \end{aligned} \quad (6)$$

where by $N(z) = \frac{2}{2-z}, \quad 0 < z \leq 1$.

3.2. Existence and Uniqueness of Solution

In this section, we present the existence and uniqueness of solution of the model system (2) using the techniques of fixed point theorem. First, we denote the Banach space of all continuous real-valued function equipped with the norm by $\mathcal{B} = \ell([0,T], \Re)$, defined as:

$$||M, S, V_1, V_2, E, I, R|| = ||M|| + ||V_1|| + ||V_2|| + ||E| + ||I|| + ||R||$$

where:

$$\begin{aligned} ||M(t)|| &= \sup_{t\in[0,T]} |M(t)|, \\ ||S|| &= \sup_{t\in[0,T]} |S(t)|, \\ ||V_1(t)|| &= \sup_{t\in[0,T]} |V_1(t)|, \\ ||V_2(t)|| &= \sup_{t\in[0,T]} |V_2(t)|, \end{aligned}$$

$$
\begin{aligned}
|E|| &= \sup_{t\in[0,T]} |E|,\\
||I(t)|| &= \sup_{t\in[0,T]} |I(t)|,\\
||R|| &= \sup_{t\in[0,T]} |R(t)|,
\end{aligned}
$$

next, we apply the non-integral operator ${}^{c}I_{0+}^{\phi}$ on both sides of the system and we get the following (2):

$$
\begin{aligned}
M(t)-M(0) &= {}^{c}I_{0+}^{z}\Big\{\Lambda-(\theta+\mu)M(t)\Big\},\\
S(t)-S(0) &= {}^{c}I_{0+}^{z}\Big\{(1-p)\theta M(t)-\\
&\quad (1-\eta)\beta S(t)I(t)-(\omega_1+\mu)S(t)\Big\},\\
V_1(t)-V_1(0) &= {}^{c}I_{0+}^{z}\Big\{p\theta M(t)+\omega_1 S(t)-\\
&\quad (1-\epsilon_1)\beta V_1(t)I(t)-(\mu+\omega_2)V_1(t)\Big\},\\
V_2(t)-V_2(0) &= {}^{c}I_{0+}^{z}\Big\{\omega_2 V_1(t)-\\
&\quad (1-\epsilon_2)\beta V_2(t)I(t)-(\mu+\gamma_2)V_1(t)\Big\},\\
E(t)-E(0) &= {}^{c}I_{0+}^{z}\Big\{(1-\eta)\beta S(t)I(t)+\\
&\quad (1-\epsilon_1)\beta V_1(t)I(t)+\\
&\quad (1-\epsilon_2)\beta V_2(t)I(t)\\
&\quad -(\mu+\alpha)E(t)\Big\},\\
I(t)-I(0) &= {}^{c}I_{0+}^{z}\Big\{\alpha E(t)-(\mu+\gamma_1)I(t)\Big\},\\
R(t)-R(0) &= {}^{c}I_{0+}^{z}\Big\{\gamma_2 V_2(t)+\\
&\quad \gamma_1 I(t)-\mu R(t)\Big\}.
\end{aligned}
\tag{7}
$$

Which implies that, for $k = 1, 2, 3..8$ we have:

$$
\begin{cases}
M(t) &= M(0)+\frac{(1-z)}{N(z)}(F_k(t,N(t))\\
&\quad +\frac{z}{N(z)}\frac{1}{\Gamma(z)}\int_0^t F_k(t,M(t))d\tau,\\
S(t) &= S(0)+\frac{(1-z)}{N(z)}(F_i(t,S(t))+\\
&\quad \frac{z}{N(z)}\frac{1}{\Gamma(z)}\int_0^t F_k(t,S(t))d\tau,\\
V_1(t) &= V_1(0)+\frac{(1-z)}{N(z)}(F_k(t,V_1(t))+\\
&\quad \frac{z}{N(z)}\frac{1}{\Gamma(z)}\int_0^t F_k(t,V_1(t))d\tau,\\
V_2(t) &= V_2(0)+\frac{(1-z)}{N(z)}(F_k(t,V_2(t))+\\
&\quad \frac{z}{N(z)}\frac{1}{\Gamma(z)}\int_0^t F_k(t,V_2(t))d\tau,
\end{cases}
\tag{8}
$$

$$
\begin{cases}
E(t) &= R_h(0)+\frac{(1-z)}{N(z)}(F_k(t,E(t))+\\
&\quad \frac{z}{N(z)}\frac{1}{\Gamma(z)}\int_0^t F_k(t,E(t))d\tau,\\
I(t) &= S_r(0)+\frac{(1-z)}{N(z)}(F_k(t,I(t))+\\
&\quad \frac{z}{N(z)}\frac{1}{\Gamma(z)}\int_0^t F_k(t,I(t))d\tau,\\
R(t) &= R(0)+\frac{(1-z)}{N(z)}(F_k(t,R(t))+\\
&\quad \frac{z}{N(z)}\frac{1}{\Gamma(z)}\int_0^t F_k(t,R(t))d\tau,
\end{cases}
\tag{9}
$$

Where:

$$
\begin{cases}
F_k(t,M(t)) &= \Lambda-(\theta+\mu)M(t),\\
F_k(t,S(t)) &= (1-p)\theta M(t)-(1-\eta)\beta S(t)I(t)-\\
&\quad (\omega_1+\mu)S(t),\\
F_k(t,V_1(t)) &= p\theta M(t)+\omega_1 S(t)-(1-\epsilon_1)\beta V_1(t)I(t)-\\
&\quad (\mu+\omega_2)V_1(t),\\
F_k(t,V_2(t)) &= \omega_2 V_1(t)-(1-\epsilon_2)\beta V_2(t)I(t)-\\
&\quad (\mu+\gamma_2)V_1(t),\\
F_k(t,M(t)) &= \Lambda-(\theta+\mu)M(t),\\
F_k(t,S(t)) &= (1-p)\theta M(t)-(1-\eta)\beta S(t)I(t)-\\
&\quad (\omega_1+\mu)S(t),\\
F_k(t,V_1(t)) &= p\theta M(t)+\omega_1 S(t)-(1-\epsilon_1)\beta V_1(t)I(t)-\\
&\quad (\mu+\omega_2)V_1(t),\\
F_k(t,V_2(t)) &= \omega_2 V_1(t)-(1-\epsilon_2)\beta V_2(t)I(t)-\\
&\quad (\mu+\gamma_2)V_1(t),\\
F_k(t,E(t)) &= (1-\eta)\beta S(t)I(t)+(1-\epsilon_1)\beta V_1(t)I(t)+\\
&\quad (1-\epsilon_2)\beta V_2(t)I(t)-(\mu+\alpha)E(t),\\
F_k(t,I(t)) &= \big(\alpha E(t)-(\mu+\gamma_1)I(t),\\
F_k(t,R(t)) &= \big(\gamma_2 V_2(t)+\gamma_1 I(t)-\mu R(t),
\end{cases}
\tag{10}
$$

The kernels N with $0 \le Q_k < 1$, satisfy the The Lipschitz condition in equation (10) holds if and only if the functions (M(t)), (S(t)), $(V_1(t))$, $(V_2(t))$, (E(t)), (I(t)), and (R(t)) are bounded above. In general, suppose that (M(t)) and . $M^*(t)$ are two functions, we have:

$$
\begin{aligned}
||F_k(t,M(t))-F_k(t,M^*(t))|| &= ||\Lambda-(\theta+\mu)M(t)\\
&\quad -\Big(\Lambda-(\theta+\mu)M^*(t)\Big)||,\\
&= \Big((\theta+\mu)\Big)||M-M^*||,\\
&\le \Big(\sup_{t\in[0,T]}\big((\theta+\mu)\big)\Big)\\
&\quad ||M-M^*||,\\
&= (\theta+\mu)||M-M^*||. \qquad (11)
\end{aligned}
$$

Where $Q_k = \alpha_h \sup_{t\in[0,T]}\big(\Lambda-(\theta+\mu)\big)$. Thus:

$$||F_k t, M(t)-F_k(t,M^*(t))|| \le Q_k||M-M^*|| \quad (12)$$

Following the results in (11) we have:

$$\begin{cases} ||F_k t, M(t) - F_k(t, M^*(t))|| & \leq Q_k||M - M^*||, \\ ||F_k t, S(t) - F_k(t, S^*(t))|| & \leq Q_k||S - S^*||, \\ ||F_k t, V_1(t) - F_k(t, V_1^*(t))|| & \leq Q_k||V_1 - V_1^*||, \\ ||F_k t, V_2(t) - F_k(t, V_2^*(t))|| & \leq Q_k||V_2 - V_2^*||, \\ ||F_k t, E(t) - F_k(t, E^*(t))|| & \leq Q_k||E - E^*||, \\ ||F_k t, I(t) - F_k(t, I^*(t))|| & \leq Q_k||I - I^*||, \\ ||F_k t, R(t) - F_k(t, R^*(t))|| & \leq Q_k||R - R^*||, \end{cases} \quad (13)$$

Whereby Q_k is the Lipschitz constant for the function $F_k(.)$ Indeed, equation (8) in recursive form as follows:

$$\begin{cases} M(t) & = M(0) + \frac{(1-z)}{N(z)} F_k(t, M_{n-1}(t)) + \\ & \frac{z}{N(z)} \frac{1}{\Gamma(z)} \int_0^t (t-\tau)^{\phi-1} F_k(\tau, M_{n-1}(\tau)) d\tau, \\ S(t) & = S(0) + \frac{(1-z)}{N(z)} F_k(t, S_{n-1}(t)) + \\ & \frac{z}{N(z)} \frac{1}{\Gamma(z)} \int_0^t (t-\tau)^{\phi-1} F_k(\tau, S_{n-1}(\tau)) d\tau, \\ V_1(t) & = V_1(0) + \frac{(1-z)}{N(z)} F_k(t, V_{1,n-1}(t)) + \\ & \frac{z}{N(z)} \frac{1}{\Gamma(z)} \int_0^t (t-\tau)^{\phi-1} F_k(\tau, V_{1,n-1}(\tau)) d\tau, \\ V_2(t) & = V_2(0) + \frac{(1-z)}{N(z)} F_k(t, V_{2,n-1}(t)) + \\ & \frac{z}{N(z)} \frac{1}{\Gamma(z)} \int_0^t (t-\tau)^{\phi-1} F_k(\tau, V_{2,n-1}(\tau)) d\tau, \\ E(t) & = E(0) + \frac{(1-z)}{N(z)} F_k(t, E_{n-1}(t)) + \\ & \frac{z}{N(z)} \frac{1}{\Gamma(z)} \int_0^t (t-\tau)^{\phi-1} F_k(\tau, E_{n-1}(\tau)) d\tau, \\ I(t) & = I(0) + \frac{(1-z)}{N(z)} F_k(t, I_{n-1}(t)) + \\ & \frac{z}{N(z)} \frac{1}{\Gamma(z)} \int_0^t (t-\tau)^{\phi-1} F_k(\tau, I_{n-1}(\tau)) d\tau, \\ R(t) & = R(0) + \frac{(1-z)}{N(z)} F_k(t, R_{n-1}(t)) + \\ & \frac{z}{N(z)} \frac{1}{\Gamma(z)} \int_0^t (t-\tau)^{\phi-1} F_k(\tau, R_{n-1}(\tau)) d\tau, \end{cases} \quad (14)$$

Suppose Ψ_k, $k = 1, 2, ..7$ be the difference between successive components in (14), We have the following:

$$\begin{cases} \Psi_n^k & = M_n(t) - M_{n-1}(t) = \frac{1-z}{N(z)} \big(F_k(t, M_{n-1}(t)) - \\ & F_k(t, M_{n-2}(t)) \big) \\ & + \frac{z}{N(z)} \frac{1}{\Gamma(z)} \int_0^t (t-\tau)^{z-1} \big(F_k(\tau, M_{n-1}(\tau)) - \\ & F_k(\tau, M_{n-2}(\tau)) \big) d\tau, \\ \Psi_n^k & = S_n(t) - S_{n-1}(t) = \frac{1-z}{N(z)} \big(F_k(t, E_{n-1}(t)) - \\ & F_k(t, S_{n-2}(t)) \big) \\ & + \frac{z}{N(z)} \frac{1}{\Gamma(z)} \int_0^t (t-\tau)^{z-1} \big(F_k(\tau, S_{n-1}(\tau)) - \\ & F_k(\tau, S_{n-2}(\tau)) \big) d\tau, \\ \Psi_n^k & = V_{1,n}(t) - V_{1,n-1}(t) = \frac{1-z}{N(z)} \big(F_k(t, V_{1,n-1}(t)) - \\ & F_k(t, V_{1,n-2}(t)) \big) \\ & + \frac{z}{N(z)} \frac{1}{\Gamma(z)} \int_0^t (t-\tau)^{z-1} \big(F_k(\tau, V_{1,n-1}(\tau)) - \\ & F_k(\tau, V_{1,n-2}(\tau)) \big) d\tau, \\ \Psi_n^k & = V_{2,n}(t) - V_{2,n-1}(t) = \frac{1-z}{N(z)} \big(F_k(t, V_{2,n-1}(t)) - \\ & F_k(t, V_{2,n-2}(t)) \big) \\ & + \frac{z}{N(z)} \frac{1}{\Gamma(z)} \int_0^t (t-\tau)^{z-1} \big(F_k(\tau, V_{2,n-1}(\tau)) - \\ & F_k(\tau, V_{2,n-2}(\tau)) \big) d\tau, \end{cases}$$

$$\begin{cases} \Psi_n^k & = E_n(t) - E_{n-1}(t) = \frac{1-z}{N(z)} \big(F_k(t, E_{n-1}(t)) - \\ & F_k(t, E_{n-2}(t)) \big) \\ & + \frac{z}{N(z)} \frac{1}{\Gamma(z)} \int_0^t (t-\tau)^{z-1} \big(F_k(\tau, E_{n-1}(\tau)) - \\ & F_k(\tau, E_{n-2}(\tau)) \big) d\tau, \\ \Psi_n^k & = I_n(t) - I_{n-1}(t) = \frac{1-z}{N(z)} \big(F_k(t, I_{n-1}(t)) - \\ & F_k(t, I_{n-2}(t)) \big) \end{cases} \quad (15)$$

$$\begin{cases} \Psi_n^k & = R_n(t) - I_{n-1}(t) = \frac{1-z}{N(z)} \big(F_k(t, R_{n-1}(t)) - \\ & F_k(t, R_{n-2}(t)) \big) \\ & + \frac{z}{N(z)} \frac{1}{\Gamma(z)} \int_0^t (t-\tau)^{z-1} \big(F_k(\tau, R_{n-1}(\tau)) - \\ & F_k(\tau, R_{n-2}(\tau)) \big) d\tau, \end{cases} \quad (16)$$

Considering that

$$\begin{cases} M_n(t) & = \sum_{p=1}^{n} \Psi_p^k(t), \\ S_n(t) & = \sum_{p=1}^{n} \Psi_p^k(t), \\ V_{1,n}(t) & = \sum_{p=1}^{n} \Psi_p^k(t), \\ V_{2,n}(t) & = \sum_{p=1}^{n} \Psi_p^k(t), \\ E_n(t) & = \sum_{p=1}^{n} \Psi_p^k(t), \\ I_n(t) & = \sum_{p=1}^{n} \Psi_p^k(t), \\ R_n(t) & = \sum_{p=1}^{n} \Psi_p^k(t). \end{cases} \quad (17)$$

Taking the norm on both sides of the equation and using equations (16) and (14), we have:

$$\begin{aligned} ||\Psi_n^k(t)|| \quad = \quad & \frac{1-\alpha}{N(\alpha)} Q_k ||Q_{n-1}^k(t)|| + \\ & \frac{\alpha}{N(\alpha)} \frac{Q_k}{\Gamma(\alpha)} \int_0^t (t-\tau)^{\alpha-1} ||Q_{n-1}^k(\tau)|| d\tau, \end{aligned} \quad (18)$$

In what follows, we state and prove the following theorem based on the results in (18).

Theorem 3.1. *The model system (2) has a unique solution for $t \in [0, T]$ if the condition below satisfies.*

$$\left(\frac{1-z}{N(z)} Q_k + \frac{1}{N(z)} \frac{Q_k}{\Gamma(z)} T^z \right) < 1, \quad k = 1, 2, ...8 \quad (19)$$

Since the function $M(t), S(t), V_1(t), V_2(t), E(t), I(t)$ and $R(t)$ are bounded and satisfy the Lipschitz condition, and using (19), we have:

$$\begin{cases} ||Q_n^k(t)|| & \leq ||M_n(0)||\left(\frac{1-z}{N(z)}Q_k + \frac{1}{N(z)}\frac{Q_k}{\Gamma(z)}T^z\right)^n, \\ ||Q_n^k(t)|| & \leq ||S_n(0)||\left(\frac{1-z}{N(z)}Q_k + \frac{1}{N(z)}\frac{Q_k}{\Gamma(z)}T^z\right)^n, \\ ||Q_n^k(t)|| & \leq ||V_{1,n}(0)||\left(\frac{1-z}{N(z)}Q_k + \frac{1}{N(z)}\frac{Q_k}{\Gamma(z)}T^z\right)^n, \end{cases} \quad (20)$$

$$\begin{cases} ||Q_n^k(t)|| & \leq ||V_{2,n}(0)||\left(\frac{1-z}{N(z)}Q_k + \frac{1}{N(z)}\frac{Q_k}{\Gamma(z)}T^z\right)^n, \\ ||Q_n^k(t)|| & \leq ||E_n(0)||\left(\frac{1-z}{N(z)}Q_k + \frac{1}{N(z)}\frac{Q_k}{\Gamma(z)}T^z\right)^n, \\ ||Q_n^k(t)|| & \leq ||I_n(0)||\left(\frac{1-z}{N(z)}Q_k + \frac{1}{N(z)}\frac{Q_{11}}{\Gamma(z)}T^z\right)^n, \\ ||Q_n^k(t)|| & \leq ||R_n(0)||\left(\frac{1-z}{N(z)}Q_k + \frac{1}{N(z)}\frac{Q_k}{\Gamma(z)}T^z\right)^n, \end{cases} \quad (21)$$

Therefore, the sequence in (21) exist, and $||Q_n^k|| \to 0$ as $n \to \infty$, $k = 1, 2, ...7$. In addition, using the triangular inequality in (21), for any s we have:

$$\begin{cases} ||M_{n+s} - M_n|| & \leq \sum_{p=n+1}^{n+s} q_k^p = \frac{q_1^{n+1} - q_k^{n+s+1}}{1-q_k}, \\ ||S_{n+s} - S_n|| & \leq \sum_{p=n+1}^{n+s} q_k^p = \frac{q_k^{n+1} - q_k^{n+s+1}}{1-q_k}, \\ ||V_{1,n+s} - V_{1,n}|| & \leq \sum_{p=n+1}^{n+s} q_k^p = \frac{q_k^{n+1} - q_k^{n+s+1}}{1-k_5}, \\ ||V_{2,n+s} - V_{2,n}|| & \leq \sum_{p=n+1}^{n+s} q_k^p = \frac{q_k^{n+1} - q_k^{n+s+1}}{1-q_k}, \\ ||E_{n+s} - E_n|| & \leq \sum_{p=n+1}^{n+s} q_k^p = \frac{q_k^{n+1} - q_k^{n+s+1}}{1-q_k}, \\ ||I_{n+s} - I_n|| & \leq \sum_{p=n+1}^{n+s} q_k^p = \frac{q_k^{n+1} - q_k^{n+s+1}}{1-q_k}, \\ ||R_{n+s} - R_n|| & \leq \sum_{p=n+1}^{n+s} q_k^p = \frac{q_k^{n+1} - q_k^{n+s+1}}{1-q_k}, \end{cases} \quad (22)$$

Where $q_k, k = 1, 2, ...7$ are the terms inside the brackets in (21). Thus, $M(t)$, $S(t)$, $V_1(t)$, $V_2(t)$, $E(t)$, $I(t)$ and $R_r(t)$ are the Cauchy sequences in $\mathcal{B}$. Therefore, one can note that as $n \to \infty$ in (14), the limit of these sequences is the unique solution of the model system (2). This completes the proofs of unique solution of the system (2).

3.3. Euler Approximation Scheme of Model (2) Using Caputo Derivative Sense

In this section, we investigate the numerical scheme for Euler fractional approximation method for the model system (2) in the sense of Caputo fractional derivatives as used in Diethelm (2010). The proposed model equations can be presented in the following form:

$$\begin{cases} {}^C D_0^z M(t) & = G_1(t, M), \\ {}^C D_0^z S(t) & = G_2(t, {}_h), \\ {}^C D_0^z V_1(t) & = G_4(t, I_h), \\ {}^C D_0^z V_2(t) & = G_5(t, R_h), \\ {}^C D_0^z E(t) & = G_3(t, W), \\ {}^C D_0^z I(t) & = G_6(t, S_r), \\ {}^C D_0^z R(t) = G_7(t, E_r), \end{cases} \quad (23)$$

Next, we present the equation (23) for $G_1(t, M)$ which satisfies the Lipschitz condition and the $M(0)$ is the initial conditions. Now applying the non-integer operator to equation (23) one can the following:

$$M(t) = M(0) + {}^C I_0^{\phi} G_1(t, M) \quad (24)$$

Where ${}^C I_0^{\phi}$ denotes the fractional integer operator with respect to the Caputo derivatives. For the proposed numerical method, we consider an interval length $[0, d]$ with time step size $h = \frac{d}{n}$ where $n \in \mathcal{N}$. Let M_k be the numerical approximation of $M(t)$ at $t = t_k$, where $t_k = 0 + kh$ and $k = 0, 1\ 2\ 3; ...n$. Applying Euler method in (24), we have the following Caputo operator formula:

$$\begin{aligned} &M_{k+1}(t) = M(0) + \frac{1-z}{N(z)}G_1(M_{Mk+1}) + \\ &\frac{h^z}{N(z)\Gamma(z)}\sum_{p=0}^{k} z_{k+1,p}G_1(M_p),\ k = 0,\ 1,\ 2, ...n-1 \end{aligned} \quad (25)$$

Where $z_{k+1,p} = (k+1-p)^z - (k-p)^z, p = 0,\ 1, ..., k$. The stability analysis of the proposed model is given by the following theorem:

Theorem 3.2. *The numerical approximation scheme (25) is conditionally stable*

Proof 3.1. *Let $\tilde{M}_0$ and $\tilde{M}_p$ be approximations of M_0 and M_p, $p = 0, ..., k+1$. From equation (25) we have:*

$$\begin{aligned} &S_{Mk+1} + \tilde{M}_{k+1} = M_0 + \tilde{M}_0 + \frac{1-z}{N(z)}G_1(M_{k+1} + \tilde{M}_{k+1}) + \\ &\frac{h^z}{N(z)\Gamma(z)}\sum_{p=0}^{k} z_{k+1,p}G_1(S_p + \tilde{M}_p) \end{aligned}$$

Using equation (25) in (26), we get:

$$\begin{aligned} |\tilde{M}_{k+1}| \quad = \quad & |M_0 + \frac{1-z}{N(z)}[G_1(M_{k+1} + \tilde{M}_{k+1}) - \\ & G_1(M_{k+1})] + \frac{\theta h^z}{N(z)\Gamma(z+1)}\sum_{p=0}^{k} z_{k+1,p}[G_1(M_p \\ & + \tilde{M}_{h_p}) - G_1(M_p)]| \end{aligned} \quad (26)$$

Applying the Lipschitz condition and triangular inequality, one get the following:

$$|\tilde{M}_{k+1}| \leq \epsilon_0 + \frac{(1-z)V_1}{N(z)}|\tilde{M}_{h_{k+1}}| + \frac{zh^z V_1}{N(z)\Gamma(z+1)}\sum_{p=0}^{k} z_{k+1,p}|\tilde{M}_p| \quad (27)$$

Where $\epsilon_0 = max_{0\leq k\leq n}\{|\tilde{M}_0| + \frac{zh^z V_1 z_{k,0}}{N(z)\Gamma(z+1)}|\tilde{M}_0|\}$ *Equation (27) can be further simplified and we get the following:*

$$|\tilde{M}_{k+1}| \leq V_1 V_{1_z}\epsilon_0 + \frac{zh^z V_1 V_{1_z}}{N(z)\Gamma(z+1)}\sum_{p=0}^{k} z_{k+1,p}|\tilde{M}_p| \quad (28)$$

Where $V_{1_z} = \frac{N(z)}{|(z-1)V_1 + N(z)|}$.

Finally, we have $|\tilde{M_{k+1}}| \leq CV_{1_z}\epsilon_0$ *and this complete the proof.*

4. Basic Properties

4.1. Positivity of Solutions

In this section, we investigate the asymptotic behavior of orbits starting in the non-negative cone $\mathbb{R}^+_8$. Obviously, system (2), which is a C^∞ differential system admits a unique maximal solution for any associated Cauchy problem. In what follows we claim the following theorem:

Theorem 4.1. *Let* $t_0 = 0$,

$$\big(X_0(t_0) = \big(M(0), S(0), V_1(0), V_2(0), E(0), I(0), R(0)\big)\big) \in \mathbb{R}^7_+$$

and for $T \in [0, +\infty]$,

$$\big([0,T], X(t) = \big(M(t), S(t), V_1(t), V_2(t), E(t), I(t), R(t)\big)\big)$$

the maximal solution of the Cauchy problem associated to system (2). Then, for all $t \in [0, T[$, $X(t) \in \mathbb{R}^7_+, \forall t \in [0, T]$.

Proof 4.1. *Let:*

$$\begin{aligned}\Delta = \{&\tilde{t} \in [0, T[, M(t) > 0, S(t) > 0, V_1(t) > 0, V_2(t) > 0,\\ &E(t) > 0, I(t) > 0, R(t) > 0 \forall t \in]0, \tilde{t}[\}.\end{aligned}$$

By continuity of functions $M(t), S(t), V_1(t), V_2(t), E(t) > 0, I(t)$ *and* $R(t)$, *one can see that* $\Delta \neq 0$. *Let* $\tilde{T} = \sup\Delta$. *next, show that* $\tilde{T} = T$. *Suppose* $\tilde{T} < T$, *then one has that* $M(t), S(t), V_1(t), V_2(t), E(t), I(t)$ *and* $R(t)$ *are non negative on* $[0, \tilde{T}[$. *At* $\tilde{T}$ *at least one of the following conditions is satisfied* $M(\tilde{T}) = 0, S(\tilde{T}) = 0, V_1(\tilde{T}) = 0, V_2(\tilde{T}) = 0, E(\tilde{T}) = 0, I(\tilde{T}) = 0$ *and* $R(\tilde{T}) = 0$. *Then, from the last equation of system (2) one has that:*

$$\frac{dM(t)}{dt} = \Lambda - (\theta + \mu)M(t). \quad (29)$$

Integrating Eq. (29) from 0 *to* $\tilde{T}$ *yields*

$$M(\tilde{T}) = M(0) + \int_0^{\tilde{T}} (\Lambda - (\theta + \mu)M(t))dt > 0.$$

Similarly, one can show that $M(\tilde{T}) > 0, S(\tilde{T}) > 0, V_1(\tilde{T}) > 0, V_2(\tilde{T}) > 0, E(\tilde{T}) > 0, I(\tilde{T}) > 0$, *and* $R(\tilde{T}) > 0$. *This is the contradiction then,* $\tilde{T} = T$ *and consequently the maximal solution* $\big(M(t), S(t), V_1(t), V_2(t), E(t), I(t), R(t)\big)$ *of the Cauchy problem associated to system (2) is positive. This completes the proof.*

4.2. Boundedness of Trajectories

In this section, We have the following result about the boundedness of trajectories of the model system (2).

Lemma 4.1. *Each non-negative solution of system (2) is bounded on* $\mathbb{R}^7_+$.

Proof 4.2. *First of all, we separate model system 2 into three parts: the human, environment and the rodent populations. Adding the first six equations of model system (2) and using equation (1), yields the following:*

$$\frac{dN(t)}{dt} \leq \Lambda - \mu N(t) \quad (30)$$

Applying the Gronwall Lemma in (30) one get the following:

$$N(t) \leq \frac{\Lambda}{\mu} + \left(N(0) - \frac{\Lambda}{\mu}\right)\exp -\mu t.$$

With this result, one has that $N(t) \leq \frac{\Lambda}{\mu}$ *for all* $t \geq 0$ *if* $N(0) \leq \frac{\Lambda}{\mu}$. *This means that:* $M \leq \frac{\Lambda}{\mu}$, $S \leq \frac{\Lambda}{\mu}$, $V_1 \leq \frac{\Lambda}{\mu}$ $V_2 \leq \frac{\Lambda}{\mu}$, $E \leq \frac{\Lambda}{\mu}$, $I \leq \frac{\Lambda}{\mu}$ *and* $R \leq \frac{\Lambda}{\mu}$. *This completes the proof.*

Corollary 4.1. *The region*

$$\begin{aligned}\Omega = \Big\{ &M, S, V_1, V_2, E, I, R) \in \mathbb{R}^7_+, M \leq \frac{\Lambda}{\mu},\\ &S \leq \frac{\Lambda}{\mu}, V_1 \leq \frac{\Lambda}{\mu}, V_2 \leq \frac{\Lambda}{\mu}, E \leq \frac{\Lambda}{\mu}, I \leq \frac{\Lambda}{\mu}, R \leq \frac{\Lambda}{\mu}\Big\},\end{aligned}$$

is invariant and attractive for system (2).

Thus, system (2) is mathematically and ecologically well posed and it is sufficient to consider the dynamics of the flow generated by system (2) in Ω.

4.3. Basic Reproduction Number and Existence of Equilibrium

In this section we use the next generation method as presented in van den Driessche & Watmough (2002) to compute the threshold quantity $\mathcal{R}_0$ which determines the persistence and extinction of disease in the population. It is believed that when the basic reproduction number $\mathcal{R}_0 > 1$ the disease persists in the population, and dies out when $\mathcal{R}_0 < 1$. The model system (2) always has a disease-free equilibrium $\mathcal{E}^0$ given by:

$$\mathcal{E}^0 : \left(M^0, S^0, V_1^0, V_2^0, E^0, I^0, R^0\right) = \left(M^*, S^*, V_1^*, , V_2^*, 0, 0, 0\right).$$

With

$$M^{0}* = \frac{\Lambda}{\mu + \theta},$$

$$
\begin{aligned}
S^* &= \frac{(1-p)\theta}{(\omega_1+\theta)(\theta+\mu)},\\
V_1 &= \frac{\Lambda\theta}{(\mu+\theta)(\omega_2+\mu)}\big(p+\frac{(1-p)\omega_1}{\omega_1+\mu}\big),\\
V_2^* &= \frac{\Lambda\theta\omega_2}{(\mu+\theta)(\omega_2+\mu)(\mu+\gamma_2)}\big(p+\frac{(1-p)\omega_1}{\omega_1+\mu}\big).
\end{aligned}
$$

Following the next generation matrix approach as used in van den Driessche & Watmough (2002), the non-negative matrix $\mathcal{F}$ that denotes the generation of new infection and the non-singular matrix $\mathcal{V}$ that denotes the disease transfer among compartments evaluated at $\mathcal{E}^0$ are defined as follows;

$$
\mathcal{F} = \begin{bmatrix} 0 & (1-\eta)\beta S^* + (1-\epsilon_1)\beta V_1^* + (1-\epsilon_2)\beta V_2^* \\ 0 & 0 \end{bmatrix} \tag{31}
$$

$$
\mathcal{V} = \begin{bmatrix} \mu+\alpha & 0 \\ -\alpha & \mu+\gamma_1 \end{bmatrix} \tag{32}
$$

Using (31) and (32) one gets the following matrix:

$$
\mathcal{M} = \begin{bmatrix} \dfrac{\alpha\left[(1-\eta)\beta S^* + (1-\epsilon_1)\beta V_1^* + (1-\epsilon_2)\beta V_2^*\right]}{(\mu+\alpha)(\mu+\gamma_1)} & \dfrac{(1-\eta)\beta S^* + (1-\epsilon_1)\beta V_1^* + (1-\epsilon_2)\beta V_2^*}{\mu+\gamma_1} \\ 0 & 0 \end{bmatrix}. \tag{33}
$$

Thus, the basic reproduction number $\mathcal{R}_0$ of the model system (2) is given by:

$$
\begin{aligned}
\mathcal{R}_0 = \frac{\alpha\beta\Lambda\theta}{(\mu+\alpha)(\mu+\gamma)(\mu+\theta)(\mu+\omega_1)}\Bigg((1-\eta)(1-p) + \\
(p\mu+\omega_1)\big((1-\epsilon_1)+\frac{(1-\epsilon_2)\omega_2}{(\omega_2+\theta)(\mu+\gamma_2)}\big)\Bigg)
\end{aligned}
$$

The basic reproduction number $\mathcal{R}_0$ is defined to be the expected number of secondary cases produced in a completely susceptible population, by one infectious individual during its lifetime.

Theorem 4.2. *If $\mathcal{R}_0 < 1$, then the DFE of system (2) is globally asymptotically stable in Ω otherwise it is unstable.*

Proof 4.3. *To prove the theorem (4.2), we evaluate the model system (2) at disease free equilibrium point E^0 and one get the following;*

$$
\begin{cases}
{}_b^cD_t^z M(t) &= M\left(\frac{\Lambda}{M^*}\big(\frac{M^*}{M}-1\big)\right),\\
{}_b^cD_t^z S(t) &= S\left(\frac{(1-p)\theta M^*}{S^*}\big(\frac{M}{M^*}\frac{S^*}{S}-1\big)-(1-\eta)\beta I\right),\\
{}_b^cD_t^z V_1(t) &= V_1\left(\frac{p\theta M^*}{V_1^*}\left(\frac{M}{M^*}\frac{V_1^*}{V_1}-1\right)+\right.\\
&\quad \left.\omega_1\frac{S^*}{V_1^*}\left(\frac{S}{S^*}\frac{V_1^*}{V_1}-1\right)-\Big(1-\epsilon_1\Big)\beta I\right),\\
{}_b^cD_t^z V_2(t) &= V_2\left(\frac{V_1^*}{V_2^*}\left(\frac{V_1}{V_1^*}\frac{V_2^*}{V_2}-1\right)-\Big(1-\epsilon_1\Big)\beta I\right),\\
{}_b^cD_t^z E(t) &= E\left(\big(1-\eta\big)\big(S-S^*\big)+\big(1-\epsilon_1\big)\big(V_1-V_1^*\big)+\right.\\
&\quad \left.\big(1-\epsilon_2\big)\big(V_2-V_2^*\big)\right)-\big(\mu+\alpha\big)E,\\
{}_b^cD_t^z I(t) &= \alpha E-\Big(\mu+\gamma_1\Big)I.
\end{cases} \tag{34}
$$

In what follows, we consider the following Lyapunov functional

$$
\begin{aligned}
\mathcal{L}_0(t) = &\left\{M(t)-M^0-M^0\ln\frac{M(t)}{M^0}\right\}+\\
&\left\{S(t)-S^0-S^0\ln\frac{S(t)}{S^0}\right\}\\
&+\left\{V_1(t)-V_1^0-V_1^0\ln\frac{V_1(t)}{V_1^0}\right\}+\\
&\left\{V_2(t)-V_2^0-V_2^0\ln\frac{V_2(t)}{V_2^0}\right\}\\
&+E(t)+\big(\frac{\mu+\alpha}{\alpha}\big)I(t).
\end{aligned} \tag{35}
$$

Lyapunov functionals have wide applications in mathematical modelling and dynamical systems, including (i) stability analysis of dynamical systems, (ii) stability and disease-control analysis in epidemiological models, and (iii) stability analysis and controller design in engineering systems. In epidemiological modelling, Lyapunov functionals are widely employed to establish the stability of disease-free and endemic equilibrium states and to investigate disease persistence or eradication. They can also be used to assess the effectiveness of vaccination and other disease-control interventions. Beyond epidemiology.

Taking the derivative of $\mathcal{L}_0(t)$ in (35) one gets the following:

$$
\begin{aligned}
{}_{t_0}^cD_t^z\mathcal{L}_0(t) \le &\left(1-\frac{M^*}{M}\right)_{t_0}^c D_t^z\mathcal{M}(t)+\\
&\left(1-\frac{S^*}{S(t)}\right)_{t_0}^c D_t^z\mathcal{S}(t)+
\end{aligned}
$$

$$\left(1-\frac{V_1^*}{V_1(t)}\right)^c_{t_0} D_t^z \mathcal{V}_1(t) + \left(1-\frac{V_2^*}{V_2(t)}\right)^c_{t_0} D_t^z \mathcal{V}_2(t) + {}^c_{t_0}D_t^z E(t) + \left(\frac{\mu+\alpha}{\alpha}\right){}^c_{t_0}D_t^z I(t) \quad (36)$$

Substituting (34) in (36) and making simplification, we have the following:

$$\begin{aligned} {}^c_b D_t^z \mathcal{L}_0(t) \leq\ & \Lambda\left(2-\frac{M}{M^*}-\frac{M^*}{M}\right) + (1-p)\theta M^*\left(1+\frac{M}{M^*}-\frac{S}{S^*}-\frac{S^*}{S}\frac{M}{M^*}\right) \\ & + p\theta M^*\left(1+\frac{M}{M^*}-\frac{V_1}{V_1^*}-\frac{M}{M^*}\frac{V_1^*}{V_1}\right) + \omega_1 S^*\left(1+\frac{S}{S^*}-\frac{V_1}{V_1^*}-\frac{V_1^*}{V_1}\frac{M}{M^*}\right) \\ & + \omega_2 V_1^*\left(1+\frac{V_1}{V_1^*}-\frac{V_2}{V_2^*}-\frac{V_2^*}{V_2}\frac{V_1}{V_1^*}\right) + \frac{(\mu+\alpha)(\mu+\gamma_1)}{\alpha}\left(\mathcal{R}_0-1\right) I \end{aligned} \quad (37)$$

*Since all the parameters and variables in system (37) are non-negative, it follows that ${}^c_b D_t^z \mathcal{L}_0(t) < 0$ holds if $\mathcal{R}_0 < 1$. Moreover, ${}^c_b D_t^z \mathcal{L}_0(t) = 0$ if and only if $M(t) = 0$, $S(t) = 0$, $V_1(t) = 0$, $V_2(t) = 0$, $E(t) = 0$, $I(t) = 0$, for all $t \geq 0$. Thus, $\mathcal{L}_0(t)$ is Lyapunov function on Ω. Using Lasalle Invariance principle **?**, implies that every solution of the system (2) approaches the DFE $\mathcal{E}^0$ as $t \to \infty$. Therefore we conclude that the DFE of system (2) is globally asymptotically stable whenever $\mathcal{R}_0 \leq 1$. This completes the proof.*

Theorem 4.3. *The Model system (2) has endemic equilibrium E^* point which is globally asymptotically stable for $\mathcal{R}_0 > 1$.*

Proof 4.4. *To prove the theorem (4.3) we consider the following Lyapunov functional:*

$$\begin{aligned} \mathcal{L}_0(t) =\ & \mathcal{B}_1\left\{M(t)-M^*-M^*\ln\frac{M(t)}{M^*}\right\} + \mathcal{B}_2\left\{S(t)-S^*-S^*\ln\frac{S(t)}{S^*}\right\} + \mathcal{B}_3\left\{V_1(t)-V_1^*-V_1^*\ln\frac{V_1(t)}{V_1^*}\right\} + \\ & \mathcal{B}_4\left\{V_2(t)-V_2^*-V_2^*\ln\frac{V_2(t)}{V_2^*}\right\} + \mathcal{B}_5\left\{E(t)-E^*-E^*\ln\frac{E(t)}{E^*}\right\} + \\ & \mathcal{B}_6\left\{I(t)-I^*-I^*\ln\frac{I(t)}{I^*}\right\} + \mathcal{B}_7\left\{R(t)-R^*-R^*\ln\frac{R(t)}{R^*}\right\}. \end{aligned} \quad (38)$$

Differentiating $\mathcal{L}_0(t)$ one gets the following

$$\begin{aligned} {}^c_{t_0} D_t^z \mathcal{L}_0(t) \leq\ & \mathcal{B}_1\left(1-\frac{M^*}{M}\right)^c_{t_0} D_t^z \mathcal{M}(t) + \mathcal{B}_2\left(1-\frac{S^*}{S(t)}\right)^c_{t_0} D_t^z S(t) + \mathcal{B}_3\left(1-\frac{V_1^*}{V_1(t)}\right)^c_{t_0} D_t^z \mathcal{V}_1(t) \\ & + \mathcal{B}_4\left(1-\frac{V_2^*}{V_2(t)}\right)^c_{t_0} D_t^z \mathcal{V}_2(t) + \mathcal{B}_5\left(1-\frac{E^*}{E(t)}\right)^c_{t_0} D_t^z \mathcal{E}(t) + \mathcal{B}_6\left(1-\frac{I^*}{I(t)}\right)^c_{t_0} D_t^z I(t) \\ & + \mathcal{B}_7\left(1-\frac{R^*}{R(t)}\right)^c_{t_0} D_t^z \mathcal{R}(t). \end{aligned} \quad (39)$$

In what follows, we substitute (2) in (39) and we get the following

$$\begin{aligned} {}^c_{t_0} D_t^z \mathcal{L}_0(t) \leq\ & \mathcal{B}_1\left(1-\frac{M^*}{M(t)}\right)\Big(\Lambda-(\theta+\mu)M(t)\Big), \\ & + \mathcal{B}_2\left(1-\frac{S^*}{S(t)}\right)\Big(ds(1-p)\theta M(t) - (1-\eta)\beta S(t)I(t) - (\omega_1+\mu)S(t)\Big), \\ & + \mathcal{B}_3\left(1-\frac{V_1^*}{V_1(t)}\right)\Big(p\theta M(t) + \omega_1 S(t) - (1-\epsilon_1)\beta V_1(t)I(t) - (\mu+\omega_2)V_1(t)\Big), \\ & + \mathcal{B}_4\left(1-\frac{V_2^*}{V_2(t)}\right)\Big(\omega_2 V_1(t) - (1-\epsilon_2)\beta V_2(t)I(t) - (\mu+\gamma_2)V_1(t)\Big), \\ & + \mathcal{B}_5\left(1-\frac{E^*}{E(t)}\right)\Big((1-\eta)\beta S(t)I(t) + (1-\epsilon_1)\beta V_1(t)I(t) + (1-\epsilon_2)\beta V_2(t)I(t) - (\mu+\alpha)E(t)\Big) + \\ & \mathcal{B}_6\left(1-\frac{I^*}{I(t)}\right)\Big(\alpha E(t) - (\mu+\gamma_1)I(t)\Big), \end{aligned}$$

$$+\mathcal{B}_7\left(1-\frac{R^*}{R(t)}\right)\left(\gamma_2 V_2(t)-\gamma_1 I(t)-\mu R(t)\right). \tag{40}$$

Let set the system (2) at the endemic equilibrium point, that is

$$\begin{cases}(\mu+\theta) & =\frac{\Lambda}{M^*},\\ (\omega_1+\mu) & =(1-p)\theta\frac{M^*}{S^*}-(1-\eta)\beta I^*,\\ (\omega_2+\mu) & =p\theta\frac{M^*}{V_1^*}+\omega_1\frac{S^*}{V_1^*}-(1-\epsilon_1)\beta I^*,\\ (\mu+\gamma_1) & =\frac{\alpha E^*}{I^*}\\ (\mu+\gamma_2) & =\omega_2\frac{V_1^*}{V_2^*}-(1-\epsilon_2)\beta I^*,\\ (\mu+\alpha) & =(1-\eta)\frac{\beta S^* I^*}{E^*}+\\ & \quad (1-\epsilon_1)\frac{\beta I^* V_1^*}{E^*}+(1-\epsilon_2)\frac{\beta I^* V_2^*}{E^*},\\ \mu & =\gamma_2\frac{V_2^*}{R^*}+\gamma_1\frac{I^*}{R^*},\end{cases} \tag{41}$$

Substituting (41) in (40) and solve the constants $\mathcal{B}_i$ with $i = 1, 2, 3..., 7$ using re-scaling method one gets the following after simplifications:

$$\begin{aligned}{}_{t_0}^{c}D_t^z\mathcal{L}_0(t) \leq\ & \frac{\Lambda}{S^*}\left(2-\frac{M}{M^*}-\frac{M^*}{M}\right)+\\ & \frac{(1-p)\theta M^*}{S^*}\left(3-\frac{S}{S^*}-\frac{M^*}{M(t)}-\frac{M}{M^*}\frac{S^*}{S}\right)\\ & +\frac{p\theta M^*}{V_1^*}\left(3-\frac{M^*}{M}-\frac{V_1}{V_1^*}\frac{M}{M^*}\frac{V_1^*}{V_1}\right)+\\ & \frac{\gamma_2 V_2^*}{R^*}\left(3-\frac{V_2}{V_2^*}\frac{R^*}{R}-\right.\\ & \left.\frac{V_1}{V_1^*}\frac{V_2^*}{V_2^*}-\frac{R}{R^*}\right)\\ & +\frac{(1-p)\theta M^*}{S^*}\left(4-\frac{M}{M^*}-\right.\\ & \left.\frac{V_1}{V_1^*}\frac{M}{M^*}\frac{S^*}{S}-\frac{S}{S^*}\frac{V_1^*}{V_1}\right)\\ & +\frac{\omega_1 V_1^*}{V_2^*}\left(4-\frac{M^*}{M}-\frac{M}{M^*}\frac{V_1^*}{V_1}-\right.\\ & \left.\frac{V_1}{V_1^*}\frac{V_2^*}{V_2}-\frac{V_2}{V_2^*}\right)\\ & +\frac{(1-\eta)\beta S^* I^*}{E^*}\left(4-\frac{M^*}{M}-\frac{M}{M^*}\frac{S^*}{S}-\right.\\ & \left.\frac{E}{E^*}\frac{I^*}{I}-\frac{S}{S^*}\frac{E^*}{E}\frac{I}{I^*}\right)\\ & +\frac{\gamma_2 V_2^*}{R^*}\left(5-\frac{M^*}{M}-\frac{M}{M^*}\frac{V_1^*}{V_1}-\right.\\ & \left.\frac{V_1}{V_1^*}\frac{V_2^*}{V_2}-\frac{V_2}{V_2^*}\frac{R^*}{R}-\frac{I}{I^*}\right)\\ & +\frac{(1-\epsilon)\beta I^* V_2^*}{E^*}\left(5-\frac{M^*}{M}-\frac{M}{M^*}\frac{V_1^*}{V_1}-\right.\\ & \left.\frac{V_1}{V_1^*}\frac{V_2^*}{V_2}-\frac{V_2}{V_2^*}\frac{E^*}{E}\frac{I}{I^*}\right).\end{aligned} \tag{42}$$

Since the arithmetic mean is greater than or equal to the geometrical mean, it follows that; from (42) one can note that ${}_{t_0}^{c}D_t^z\mathcal{L}_0(t) \leq 0$ whenever $\mathcal{R}_0 > 1$. Therefore by using Lasalle Invariance principle LaSalle (1976), the system (2) have global asymptotically stable equilibrium point for all $\mathcal{R}_0 > 1$ and this completes the proof.

5. Results and Discussion

Adam-Bashforth-Moulton scheme and Euler algorithm have been used in numerical simulation of fractional-order systems. We use the same approach to perform the numerical simulation of the studied fractional model and investigate the solution behavior of the system. For simulation purpose, we set the initial condition of variable to be: $M(0) = 10$, $S(0) = 500$, $E(0) = 2$, $I(0) = 1$, $S_1(0) = 1$, $V_2(0) = 1$, and $R(0) = 20$. Additional, some of the model parameters used in simulations have been estimated using real data of Monkey pox disease reported in the literature and some have been drawn from published documents as shown in Table 1.

5.1. Model Parameter Estimations

In this part, we conduct the model fitting and parameter estimation using the root-mean square error (RMSE) and assess the validity of model in predicting dynamics of disease in the population. We fitted the model using real data from Democratic Republic of Congo (DRC) and estimated the parameters using the formula presented in (43):

$$\text{RMSE} = \sqrt{\frac{1}{n}\sum_{k=1}^{28}(I(k)-\hat{I}(k))^2}, \tag{43}$$

Where n denotes the number of infections reported for 28 months. For simulation purposes, we set the initial value of variables to be: $M(0) = 10$, $S(0) = 500$, $E(0) = 2$, $I(0) = 1$, $S_1(0) = 1$, $V_2(0) = 1$, and $R(0) = 20$. Furthermore, we use the following formula to generated the new number of infections for both fractional model at $z = 0.52$ and classical integer model at $z = 1$: $\beta I(t)\big((1-\eta)S(t)+(1-\epsilon_1)V_1(t)+(1-\epsilon_2)V_2(t)\big)$ and the results are presented in Figure (3).

Table 1
Definition of model parameters and values

Symbol	Definition	Value	Units	Source
β	Disease transmission from human to human	7.45×10^{-10}	day^{-1}	Bhunu & Mushayabasa (2011)
μ	Natural mortality rate of human	0.01428	day^{-1}	Bhunu & Mushayabasa (2011); Peter et al. (2022)
ω_1	First dose vaccination for susceptible humans	0.002	$[0, 1]$	Varied
ω_2	Second dose vaccination for susceptible humans	0.002	$[0, 1]$	Varied
α	Progression rate from incubation to infectious	0.25	day^{-1}	Peter et al. (2022)
γ_2	Progression rate of vaccinated humans to recovered	0.99	day^{-1}	Peter et al. (2022)
γ_1	Progression rate from infectious to recovered	0.94	day^{-1}	Peter et al. (2022)
Λ	Recruitment rate of humans	0.029	day^{-1}	Bhunu & Mushayabasa (2011); Peter et al. (2022)
η	Rate of human awareness	$[0, 1]$	day^{-1}	Fitted
ϵ_1	Efficacy of first dose vaccination	$[0, 1]$	day^{-1}	Varied
ϵ_2	Efficacy of second dose vaccination	$[0, 1]$	day^{-1}	Varied
μ_v	Natural decay of virus in environment	0.0939	day^{-1}	Peter et al. (2022)
θ	Proportion of newborn babies	$[0, 1]$	day^{-1}	Fitted
p	Newborn babies with immunity	$[0, 1]$	day^{-1}	Fitted

Figure 3: *Single-column presentation of model fits and numerical results for monkeypox.*

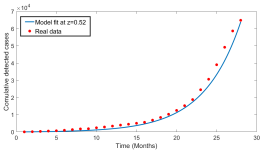

(a) Fractional model fit to the real data of monkeypox at $z = 0.52$

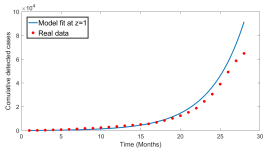

(b) Classical model fit to the real data of monkeypox at $z = 1.0$

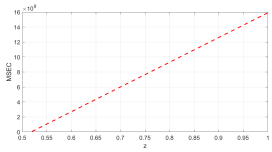

(c) Numerical results of varying order of derivatives versus cumulative Mean Square Error

Numerical results in Figure (3) show the fractional and classical model fit o the real data of monkey pox disease in Democratic Republic of Congo. The parameter values used in simulations are estimated and presented in Table (1). Note that the order of derivative is denoted by $z \in (0, 1]$ with $0 < z < 1$ represent the fractional model and classical integer when $z = 1$. Overall, the results showed that model fit with $z = 0.52$ had accurate results compared to $z = 1$, implies that the fractional model had best fit to real data of monkey pox compared to classical integer model. Additional, results in Figure 3(b) show that as the order of derivatives increase from 0.52 to 1 the mean square error commutative increases imply that classical integer model had higher mean square error compared to fractional model.

Figure 4: *Sensitivity analysis of the $\mathcal{R}_0$ to the model parameters*

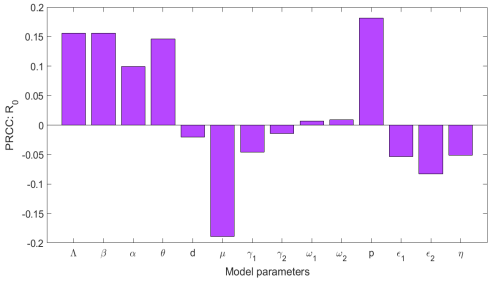

Figure (4) shows the relationship between model model parameters and $\mathcal{R}_0$. We generated the numerical results using Partial Rank Correlation Coefficient (PRCC) and investigate the effects of model parameters on the $\mathcal{R}_0$. The numerical results show that parameters such as: Λ, β, α, θ, p, ω_1 and ω_2 have positive indices with $\mathcal{R}_0$. On the other-hand, model parameters such as: d, μ, γ_1, γ_2, ϵ_1, ϵ_2 and η have negative indices with $\mathcal{R}_0$. Implies that increase one the new recruitment of humans and new born babies with less immunity increases the spread of disease in the population. In contrast, the result demonstrated that increase on sensitization campaigns of health education and vaccine efficacy reduce the spread of disease in the population.

Figure 5: *Numerical simulation of: (a) Latin Hypercube sampling of $\mathcal{R}_0$ and rate of disease transmission between humans, (b) Latin Hypercube sampling of $\mathcal{R}_0$ and efficacy of first dose vaccination, (c) Latin Hypercube sampling of $\mathcal{R}_0$ and efficacy of second dose vaccination, (d) Latin Hypercube sampling of $\mathcal{R}_0$ and rate of human awareness on monkeypox disease transmission, (e) Latin Hypercube sampling of $\mathcal{R}_0$ and first dose vaccination, (f) Latin Hypercube sampling of $\mathcal{R}_0$ and second dose vaccination.*

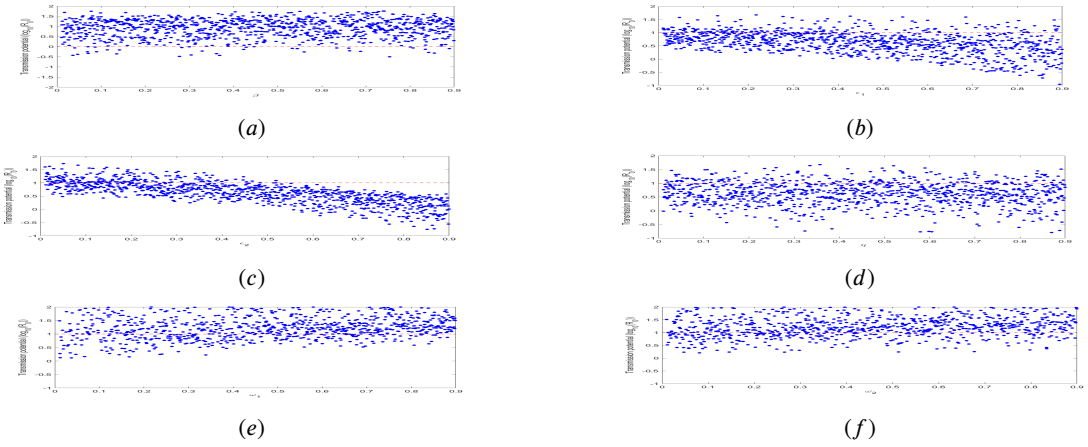

In Figure (5), we Simulation of Latin Hypercube sampling of $\mathcal{R}_0$ versus the key parameters of the model and investigate their influence on spread of disease in the population. We generated the results using parameters presented in Table (1). We observed that parameter such as probability of disease transmission β, rate of first dose vaccination ω_1 and second dose vaccination ω_2 correlated positively with $\mathcal{R}_0$. On the otherhand, model parameters such as rate of human awareness η, efficacy of first dose vaccination ϵ_1 and efficacy of second dose vaccination ϵ_2 correlated negatively with $\mathcal{R}_0$. In disease mitigation, increase on human awareness, efficacy of first and second dose vaccination lead to decrease on the disease transmission to human within the population. In contrast, increase on the contact rate between susceptible and infected individuals lead to increase of disease transmission in the population. Numerical simulation in Figure (6) demonstrates

Figure 6: *Contour plots of $\mathcal{R}_0$: (a) as a function of efficacy of first-dose vaccination (ϵ_1) and health education campaigns (η); (b) as a function of efficacy of first-dose vaccination (ϵ_1) and efficacy of second-dose vaccination (ϵ_2).*

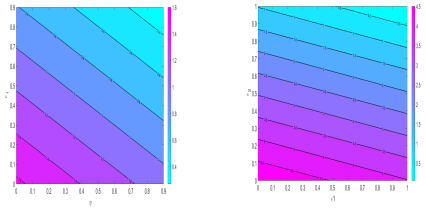

Contour plots of $\mathcal{R}_0$ (a) as the function of efficacy of first dose vaccination (ϵ_1) and health education campaigns η (b) as the function of efficacy of first dose vaccination (ϵ_1) and efficacy of second dose vaccination (ϵ_2). Overall,One can note that implementing first dose vaccination with high efficacy (ϵ_1) along with health education campaign (η) reduce the size of $\mathcal{R}_0$. The results have imply that policy markers and other stake holder must put effort on health education campaigns and allocate enough resources for implementing vaccination to susceptible humans. Additional, the results showed that implementing first and second dose vaccination with high efficacy the disease dies in the population In Figure

Figure 7: *Dynamical solution of model 2 at $\mathcal{R}_0 < 1$. The values of model parameters used in generating the results are presented in Table 1, and the orders of derivatives were selected within the reasonable range and set to be $z = 0.3,\ 0.5,\ 0.7,\ 0.9,\ 1$: (a) shows the dynamical solution behavior of susceptible humans, (b) describes the dynamical solution behavior of recovered humans, (c) shows the solution behavior of individuals receiving second-dose vaccinations, (d) shows the dynamical solution behavior of humans receiving first-dose vaccinations, (e) shows the numerical solution behavior of infected humans, and (f) shows the numerical solution behavior of exposed humans.*

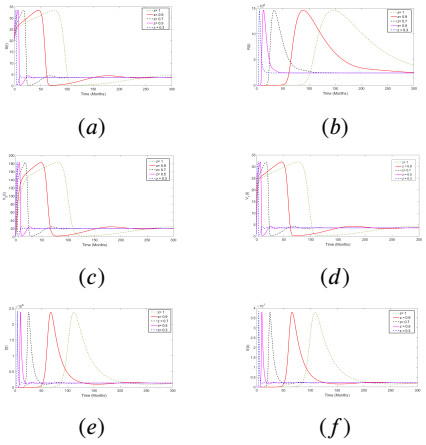

(7) we performed numerical simulation of model system (2) and investigate the impact of memory effects on the spread of disease in the population. We varied the order of derivatives $z \in (01]$ with $0 < z \leq 1$ represent the fractional model and classical integer model when $z = 1$. We have observed that as the order of derivative z approaches 0 (in particular $z = 0.3$) the solution behavior increases at beginning and converge to the equilibrium point after 20 months of infections. On the other-hand, as the order of derivative z approaches 1 the model solutions increase at the beginning and converge to the disease after 200 months of infections. Implies that as the order of derivative approaches 0 the system retain the memory for long time and loose faster when the order of derivatives approaches 1. In

Figure 8: *Numerical solutions of model system 2 at $\mathcal{R}_0 > 1$. The values of model parameters used in the simulations are presented in Table 1, and the order of derivatives was selected within the reasonable range and set to be $z = 0.3,\ 0.5,\ 0.7,\ 0.9,\ 1$: (a) solution behavior of susceptible humans, (b) dynamical solution of recovered individuals, (c) solution behavior of individuals receiving second-dose vaccinations, (d) solution behavior of humans receiving first-dose vaccinations, (e) numerical solution behavior of infected humans, (f) numerical solution behavior of exposed humans.*

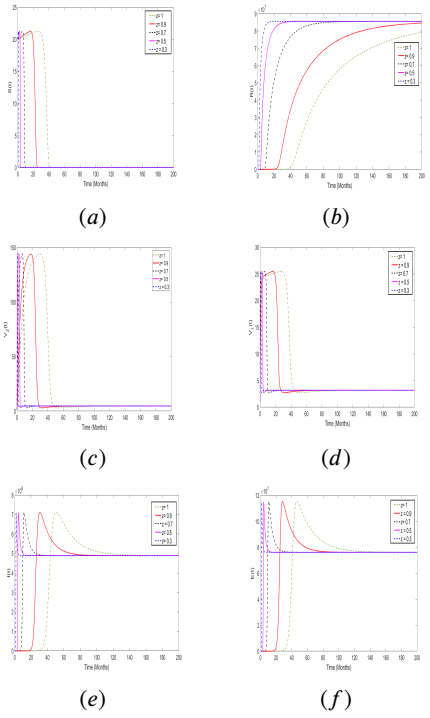

Figure (8) assess the impact of memory effects on the spread of monkey pox disease $\mathcal{R}_0 > 1$, we performed the numerical simulation of the model system (2) by varying the order of derivative within the reasonable range and was set to be $z = 0.3,\ z = 0.5,\ z = 0.7,\ z = 0.9,\ z = 1$. It was observed that, the numerical results increase at the beginning, followed by sharp decrease and converge to the unique equilibrium point. In particular, we noted that the model solutions fractional-order attain its stability much faster compared to the solution of integer derivative. The results have implication that as the order of derivative approaches 0 the biological species retain its memory for long time compared to when the order of derivative approaches unity.

5.2. *Effects of Human Awareness on the Disease Dynamics*

Figure 9: *Numerical results of the model system (2) to assess the effects of health education campaigns on Monkeypox disease transmission: (a) solution behavior of infected humans, (b) dynamical behavior of exposed individuals, (c) solution behavior of individuals receiving first-dose vaccination, (d) solution behavior of humans receiving second-dose vaccination, (e) numerical solution of susceptible humans, and (f) solution behavior of recovered humans.*

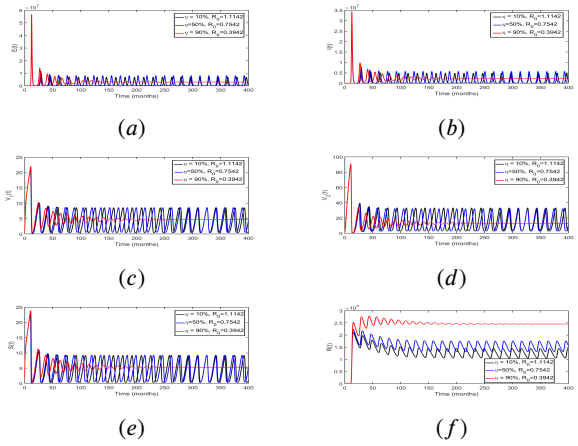

In Figure (9) we conducted the numerical simulation of the model system (2) to investigate the effects of community awareness on reduce the monkey pox disease transmission. The model parameters used in generating results are presented in Table (1) and the initial condition of variables were assigned to be: $M(0) = 10$, $S(0) = 500$, $E(0) = 2$, $I(0) = 1$, $S_1(0) = 1$, $V_2(0) = 1$, and $R(0) = 20$. Additionally, the rate of human awareness were selected to be $\eta = 0.1$ $\eta = 0.5$, $\eta = 0.9$. Overall, the results showed that, health education have impact in reduce the spread of Monkey pox in the population. In particular, we noted that implementing health education below 50% the disease remain endemic in the population. In contrast, we observed that when the rate of human awareness become greater than 0.5 the threshold quantity $\mathcal{R}_0$ become less than unity. This has implication that, to eliminate the disease policy markers and other stake holders must allocate enough resource to implement health education campaigns in the community.

Figure 10: *Dynamical behavior of the model system (2) to investigate the impact of first-dose vaccination and health education campaigns on disease transmission: (a) dynamical behavior of infected humans, (b) solution behavior of exposed individuals, (c) solution behavior of individuals receiving first-dose vaccination, and (d) solution behavior of recovered humans.*

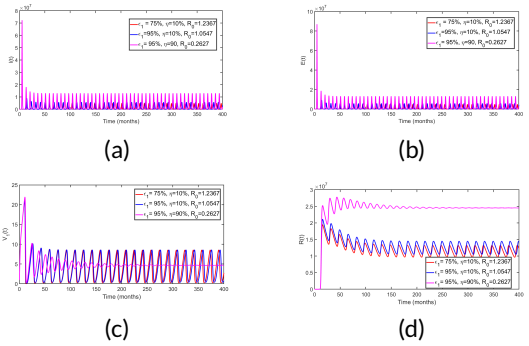

5.3. *Effects of First Dose Vaccination and Human Awareness on the Disease Dynamics*

In Figure (10), we perform numerical simulation of the model system (2) to investigate the combined effect first-dose vaccination and awareness on minimize the spread monkey pox disease in the population. We simulated the results using model parameters presented in Table (1) and the initial condition of variables were assumed to be: $M(0) = 10$, $S(0) = 500$, $E(0) = 2$, $I(0) = 1, S_1(0) = 1, V_2(0) = 1$, and $R(0) = 20$. The results showed that: (i) when the efficacy of first-dose vaccine is 75% and rate of human awareness is 0.1, the value of threshold quantity $\mathcal{R}_0$ remains greater than unity, (ii) when the efficacy of first-dose vaccine changed from 75% to 95% while the rate of human awareness retained at 0.1 the disease remained endemic in the population, (iii) when the efficacy of first-dose vaccine changed from 75% to 95% and rate of human awareness varied from 0.1 to 0.9 the value of threshold quantity become less than unity. The results have implication that, for the disease elimination first-dose vaccination must be implemented at 95% while the level of human awareness on how to prevent themselves with monkey pox disease must be greater than 90%. Numerical results in Figure (11) shows the dynamical behavior of the model system (2). We performed the simulations to assess the combined effect first and second dose vaccination on minimize the spread monkey pox disease in the community. It was observed that: (i) when the efficacy of first-dose vaccine is 75% and that of second-dose vaccination is 95%, the value of threshold quantity $\mathcal{R}_0$ is greater than unity, (ii) when the efficacy of first-dose vaccine is 75% and the efficacy of second-dose vaccination is changed from 95% to 99% the value of threshold quantity, $\mathcal{R}_0$ remained greater than unity, (iii) when the efficacy of first-dose vaccine changed from 75% to 95% and that of second-dose varied from 95% to 99% the value of threshold quantity become less than unity. The results concur with the one obtained in figure (10), imply that the efficacy of first-dose vaccine must be greater than 95% for the disease to be eliminated in the population.

5.4. *Effects of First and Second Dose Vaccination on the Disease Dynamics*

Figure 11: Dynamical behavior of the model system (2) to assess the effects of first-dose and second-dose vaccination on monkeypox disease transmission: (a) infected humans, (b) exposed individuals, (c) first-dose vaccinated individuals, (d) second-dose vaccinated individuals, (e) susceptible humans, and (f) recovered humans.

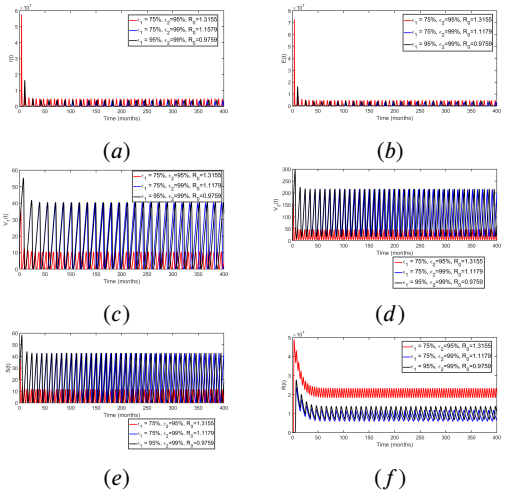

5.5. *Effects of Maternal Immunization on the Disease Dynamics*

Figure 12: *Numerical simulations of the model system (2) to assess the impact of maternal immunizations on disease transmission: (a) dynamical behavior of infected humans, (b) solution behavior of exposed individuals, (c) solution behavior of first-dose vaccinated individuals, (d) solution behavior of second-dose vaccinated individuals, (e) solution behavior of susceptible humans, and (f) solution behavior of recovered humans.*

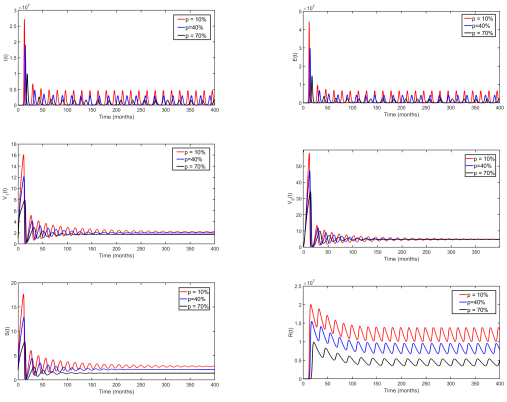

6. Conclusion and Recommendations

In this research work, we formulated and studied a fractional-order model to study the dynamics of Monkeypox virus transmission, and investigation the impact of health education campaigns and vaccinations. In model analysis the disease-free equilibrium and basic reproduction number were computed using the next-generation method. The Sensitivity analysis on the basic reproduction number was performed using partial rank correlation coefficients to explore the influence of each parameter on the disease transmission. Overall, the results presented graphically showing both the negative and positive indices, and it was observed that increasing parameters with negative indices led to a decrease in the reproduction number, whereas increasing parameters with positive indices the disease persists in the population. Furthermore, calibration of the model using real data of Monkeypox from Democratic Republic of Congo was conducted to compare the results for fractional and integer-order model. It was observed that, fitting fractional-order model ($z = 0.5$) provided better results compared to integer-order model ($z = 1$). This results imply that modeling biological system using fractional-order model provide best results compared to integer models. Furthermore, we performed numerical simulation of the model at $\mathcal{R}_1 < 1$ and $\mathcal{R}_1 > 1$ to assess the impact of memory effects, we simulated the model at the order of derivative $z = 0.3, z = 0.5, z = 0.7, z = 0.9$ and $z = 1$. The results showed that, as the order of derivatives approached zero, the model solution attain its stability much faster compared to when approaching unity. This suggests that as the derivatives approaches 0 biological species retain its memory for long time compared to when the order of derivatives is close to 1. Finally, we simulated the model to assess the impact of health education campaigns and vaccination. Overall, the results showed that, health education have impact in reduce the spread of Monkey pox in the population. In particular, we noted that implementing health education below 50% the disease remain endemic in the population. In contrast, we observed that when the rate of human awareness is greater than 0.5 the disease dies in the population. Furthermore, we numerically investigated the effects of vaccination on spread of disease in the population. It was observed that: (i) when the efficacy of first-dose vaccine is 75% and that of second-dose vaccination is 95%, the value of threshold quantity $\mathcal{R}_0$ is greater than unity, (ii) when the efficacy of first-dose vaccine is 75% and the efficacy of second-dose vaccination is changed from 95% to 99% the value of threshold quantity, $\mathcal{R}_0$ remained greater than unity, (iii) when the efficacy of first-dose vaccine changed from 75% to 95% and that of second-dose varied from 95% to 99% the value of threshold quantity become less than unity. The results suggesting that the first-dose vaccine must be greater than 95% for the disease to be eliminated in the population. However, future improvements to the model could consider the interaction between humans, wild animals and environment. Furthermore, the model can consider the effects of humans and wild animal migrations on the dynamics of Monkeypox virus transmission.

7. Acknowledgements

The authors would like to express their sincere gratitude to all individuals and institutions whose support and contributions facilitated the successful completion of this study.

8. References

Addai, E., Ngungu, M., Omoloye, M. A., Marinda, E., et al. (2023). Modelling the impact of vaccination and environmental transmission on the dynamics of monkeypox virus under Caputo operator. *Mathematical Biosciences and Engineering*, *20*, 10174–10199.

Adel, W., Elsonbaty, A., Aldurayhim, A., & El-Mesady, A. (2023). Investigating the dynamics of a novel fractional-order monkeypox epidemic model with optimal control. *Alexandria Engineering Journal*, *73*, 519–542.

Adepoju, O., & Ibrahim, H. (2024). An optimal control model for monkeypox transmission dynamics with vaccination and immunity loss following recovery. *Healthcare Analytics*, *6*, 100355.

Alakunle, E., Moens, U., Nchinda, G., & Okeke, M. I. (2020). Monkeypox virus in Nigeria: Infection biology, epidemiology, and evolution. *Viruses*, *12*, 1257.

Alqahtani, R. T., Musa, S. S., & Inc, M. (2023). Modeling the role of public health intervention measures in halting the transmission of monkeypox virus. *AIMS Mathematics*, *8*, 14142–14166.

Alshehri, A., & Ullah, S. (2023). Optimal control analysis of monkeypox disease with the impact of environmental transmission. *AIMS Mathematics*, *8*, 16926–16960.

Ayeh, M. A., Cofie, K., Mensah, G. S., Amo-Kodieh, F., Kyeremeh, P., et al. (2024). Monkeypox infection: Risk assessment and clinical outcomes among immunocompromised populations in Sub-Saharan Africa: A systematic review and meta-analysis. *Ghana Journal of Nursing and Midwifery*, *1*, 107–124.

Banuet-Martinez, M., Yang, Y., Jafari, B., Kaur, A., Butt, Z. A., Chen, H. H., Yanushkevich, S., Moyles, I. R., Heffernan, J. M., Korosec, C. S., et al. (2023). Monkeypox: A review of epidemiological modelling studies and how modelling has led to mechanistic insight. *Epidemiology & Infection*, *151*, e121.

Bhunu, C., & Mushayabasa, S. (2011). Modelling the transmission dynamics of pox-like infections. *IAENG International Journal*.

Biswas, S. A., Aslam, B. H., & Tiwari, P. K. (2023). Mathematical modeling of a novel fractional-order monkeypox model using the Atangana–Baleanu derivative. *Physics of Fluids*, *35*.

Brand, S. P., Cavallaro, M., Cumming, F., Turner, C., Florence, I., Blomquist, P., Hilton, J., Guzman-Rincon, L. M., House, T., Nokes, D. J., et al. (2023). The role of vaccination and public awareness in forecasts of mpox incidence in the United Kingdom. *Nature Communications*, *14*, 4100.

Caputo, M. (1967). Linear models of dissipation whose Q is almost frequency independent. *Geophysical Journal International*, *13*, 529–539.

Di Gennaro, F., Veronese, N., Marotta, C., Shin, J. I., Koyanagi, A., Silenzi, A., Antunes, M., Saracino, A., Bavaro, D. F., Soysal, P., et al. (2022). Human monkeypox: A comprehensive narrative review and analysis of the public health implications. *Microorganisms*, *10*, 1633.

Diethelm, K. (2010). *The Analysis of Fractional Differential Equations*. Springer.

van den Driessche, P., & Watmough, J. (2002). Reproduction numbers and sub-threshold endemic equilibria for compartmental models of disease transmission. *Mathematical Biosciences*, *180*, 29–48.

El-Mesady, A., Elsonbaty, A., & Adel, W. (2022). On nonlinear dynamics of a fractional-order monkeypox virus model. *Chaos, Solitons & Fractals*, *164*, 112716.

Farman, M., AkgÃijl, A., Garg, H., Baleanu, D., Hincal, E., Shahzeen, S., et al. (2025). Mathematical analysis and dynamical transmission of monkeypox virus model with fractional operator. *Expert Systems*, *42*, e13475.

Ghanbari, B., & Atangana, A. (2020). A new application of fractional Atangana–Baleanu derivatives: Designing ABC-fractional masks in image processing. *Physica A*, *542*, 123516.

Hatami, H., Jamshidi, P., Arbabi, M., Safavi-Naini, S. A. A., Farokh, P., Izadi-Jorshari, G., Mohammadzadeh, B., Nasiri, M. J., Zandi, M., Nayebzade, A., et al. (2023). Demographic, epidemiologic, and clinical characteristics of human monkeypox disease pre- and post-2022 outbreaks: A systematic review and meta-analysis. *Biomedicines*, *11*, 957.

Helikumi, M., Bisaga, T., Makau, K. A., & Mhlanga, A. (2024). Modeling the impact of human awareness and insecticide use on malaria control: A fractional-order approach. *Mathematics*, *12*, 3607.

Helikumi, M., & Lolika, P. O. (2022). Global dynamics of fractional-order model for malaria disease transmission. *Asian Research Journal of Mathematics*, *18*, 82–110.

Helikumi, M., & Mushayabasa, S. (2023). Mathematical modeling of trypanosomiasis control strategies in communities where human, cattle and wildlife interact. *Animal Diseases*, *3*, 25.

Helikumi, M., Ojija, F., & Mhlanga, A. (2025). Dynamical analysis of mpox disease with environmental effects. *Fractal and Fractional*, *6*, 356.

Khan, A., Sabbar, Y., & Din, A. (2022). Stochastic modeling of the monkeypox 2022 epidemic with cross-infection hypothesis in a highly disturbed environment. *Mathematical Biosciences and Engineering*, *19*, 13560–13581.

LaSalle, J. (1976). *The Stability of Dynamical Systems*. SIAM, Philadelphia.

Liu, B., Farid, S., Ullah, S., Altanji, M., Nawaz, R., & Teklu, S. W. (2023). Mathematical assessment of monkeypox disease with the impact of vaccination using a fractional epidemiological modeling approach. *Scientific Reports*, *13*, 13550.

Lusekelo, E., Helikumi, M., Kuznetsov, D., & Mushayabasa, S. (2022). Modeling the effects of temperature and heterogeneous biting exposure on chikungunya virus disease dynamics. *Informatics in Medicine Unlocked*, *32*, 101007.

Lusekelo, E., Helikumi, M., Kuznetsov, D., & Mushayabasa, S. (2023). Dynamic modelling and optimal control analysis of a fractional order chikungunya disease model with temperature effects. *Results in Control and Optimization*, *10*, 100206.

Mandja, B. A. M., Brembilla, A., Handschumacher, P., Bompangue, D., Gonzalez, J. P., Muyembe, J. J., & Mauny, F. (2019). Temporal and spatial dynamics of monkeypox in Democratic Republic of Congo, 2000–2015. *EcoHealth*, *16*, 476–487.

Mandja, B. A. M., & Gonzalez, J. P. (2025). Monkeypox disease epidemiology and virus ecology: From neglected to high consequence infectious disease. IntechOpen.

McKenzie, H. W., Jin, Y., Jacobsen, J., & Lewis, M. A. (2012). R_0 analysis of a spatiotemporal model for a stream population. *SIAM Journal on Applied Dynamical Systems*, *11*, 567–596.

Musafir, R. R., Suryanto, A., & Darti, I. (2024). Optimal control of a fractional order monkeypox epidemic model with vaccination and rodents culling. *Results in Control and Optimization*, *14*, 100381.

Nisar, K. S., Farman, M., Abdel-Aty, M., & Ravichandran, C. (2024). A review of fractional order epidemic models for life sciences problems: Past, present and future. *Alexandria Engineering Journal*, *95*, 283–305.

Peter, O. J., Abidemi, A., Ojo, M. M., & Ayoola, T. A. (2023). Mathematical model and analysis of monkeypox with control strategies. *The European Physical Journal Plus*, *138*, 242.

Peter, O. J., Kumar, S., Kumari, N., Oguntolu, F. A., Oshinubi, K., & Musa, R. (2022). Transmission dynamics of monkeypox virus: A mathematical modelling approach. *Modeling Earth Systems and Environment*, 1–12.

Podlubny, I. (1999). *Fractional Differential Equations*. Academic Press, San Diego.

Rakkiyappan, R., Latha, V. P., & Rihan, F. A. (2019). A fractional-order model for Zika virus infection with multiple delays. *Complexity*, 4178073.

Rashid, S., Bariq, A., Ali, I., Sultana, S., Siddiqa, A., & Elagan, S. K. (2025). Dynamic analysis and optimal control of a hybrid fractional monkeypox disease model in terms of external factors. *Scientific Reports*, *15*, 2944.

Soni, K., & Sinha, A. K. (2024). Modeling and stability analysis of the transmission dynamics of monkeypox with control intervention. *Partial Differential Equations in Applied Mathematics*, *10*, 100730.

Spath, T., Brunner-Ziegler, S., Stamm, T., Thalhammer, F., Kundi, M., Purkhauser, K., & Handisurya, A. (2022). Modeling the protective effect of previous compulsory smallpox vaccination against human monkeypox infection: From hypothesis to worst-case scenario. *International Journal of Infectious Diseases*, *124*, 107–112.

Vargas-De-LeÃşn, C. (2015). Volterra-type Lyapunov functions for fractional order epidemic systems. *Communications in Nonlinear Science and Numerical Simulation*, *24*, 75–85.

Venkatesh, A., Manivel, M., Arunkumar, K., Prakash Raj, M., Shyamsunder, P., & Purohit, S. (2024). A fractional mathematical model for vaccinated humans with the impairment of monkeypox transmission. *European Physical Journal Special Topics*, 1–21.

Yaga, S. J. (2025). Modeling monkeypox epidemics: Thresholds, temporal dynamics, and waning immunity from smallpox vaccination.

Yuan, P., Tan, Y., Yang, L., Aruffo, E., Ogden, N. H., BÃl'lair, J., Arino, J., Heffernan, J., Watmough, J., & Carabin, H. (2022). Modeling vaccination and control strategies for outbreaks of monkeypox at gatherings. *Frontiers in Public Health*, *10*, 1026489.